Published in final edited form as:
Biomaterials. 2009 February ; 30(5): 859–866. doi:10.1016/j.biomaterials.2008.09.056.

Single-Step Surface Functionalization of Polymeric Nanoparticles for Targeted Drug Delivery

Yogesh Patil[1,2], **Udaya Toti**[2], **Ayman Khdair**[1,2], **Linan Ma**[3], and **Jayanth Panyam**[3,*]

1 *Department of Pharmaceutical Sciences, Eugene Applebaum College of Pharmacy and Health Sciences, Wayne State University, Detroit, MI 48201*

2 *Department of Pharmaceutics, University of Minnesota, Minneapolis, MN 55455*

3 *Masonic Cancer Center, Minneapolis, MN 55455*

Abstract

Targeted drug delivery using nanocarriers is achieved by functionalizing the carrier surface with a tissue-recognition ligand. Current surface modification methods require tedious and inefficient synthesis and purification steps, and are not easily amenable to incorporating multiple functionalities on a single surface. In this report, we describe a versatile, single-step surface functionalizing technique for polymeric nanoparticles. The technique utilizes the fact that when a diblock copolymer like polylactide-polyethylene glycol (PLA-PEG) is introduced in the oil/water emulsion used in polymeric nanoparticle formulation, the PLA block partitions into the polymer containing organic phase and PEG block partitions into the aqueous phase. Removal of the organic solvent results in the formation of nanoparticles with PEG on the surface. When a PLA-PEG-ligand conjugate is used instead of PLA-PEG copolymer, this technique permits a 'one-pot' fabrication of ligand-functionalized nanoparticles. In the current study, the IAASF approach facilitated the simultaneous incorporation of biotin and folic acid, known tumor-targeting ligands, on drug-loaded nanoparticles in a single step. Incorporation of the ligands on nanoparticles was confirmed by using NMR, surface plasmon resonance, transmission electron microscopy and tumor cell uptake studies. Simultaneous functionalization with both ligands significantly enhanced nanoparticle accumulation in tumors *in vivo*, and resulted in greatly improved efficacy of paclitaxel-loaded nanoparticles in a mouse xenograft tumor model. This new surface functionalization approach will enable the development of targeting strategies based on the use of multiple ligands on a single surface to target a tissue of interest.

Keywords

Targeted delivery; surface functionalization; chemotherapy; polymeric systems; multivalent

1. Introduction

An important goal in drug therapy is to enhance the availability of drug at its site of action while minimizing its exposure to non-target sites. Polymeric nanoparticles have emerged as a versatile carrier system for targeted delivery of small molecular weight drugs as well as

* Author for correspondence: Department of Pharmaceutics, College of Pharmacy, University of Minnesota, 308 Harvard Street SE, Minneapolis, MN 55455, Phone: 612-624-0951, Fax: 612-626-2215, Email: jpanyam@umn.edu.

macromolecular therapeutic agents to the tissue of interest [1-3]. Use of polymeric materials in nanoparticle fabrication permits the slow release of the drug molecule for sustained therapeutic effect. Surface functionalization of nanoparticles with hydrophilic polymers such as polyethylene glycol (PEG) increases the residence time of nanoparticles in the systemic circulation while inclusion of tissue-recognition ligands enables targeted delivery [4-7].

Current methods of incorporating ligands on the surface of nanoparticles usually involve chemical conjugation of the ligand to pre-synthesized nanoparticles [8-10]. Chemical conjugation to preformed particles is not useful if the material used for nanoparticle fabrication lacks reactive functional groups or if the reaction conditions are detrimental to the payload. Further, chemical conjugation involves addition of pre-formed nanoparticles to a liquid reaction medium, which may result in the loss of payload from nanoparticles. Chemical coupling of ligand to nanoparticles can be expensive and time consuming because the chemistry needs to be optimized for each polymer-ligand combination and may need to be modified based on the properties of the encapsulated drug. Importantly, introduction of multiple ligands on the surface requires tedious and inefficient sequential synthesis and purification steps.

In this report, we describe a facile, single-step surface functionalization technique driven by interfacial activity of block copolymers. When an amphiphilic diblock copolymer is introduced into an oil/water biphasic system, the hydrophobic block tends to partition into the oil phase while the hydrophilic block remains in the aqueous phase (Figure 1A). In the proposed approach, polymer to be used in nanoparticle fabrication and drug of interest are first dissolved in an organic solvent like chloroform; this polymer-drug solution is emulsified in an aqueous solution containing a surfactant such as polyvinyl alcohol. The desired ligands are conjugated to the hydrophilic end of an amphiphilic diblock copolymer like polylactide-polyethylene glycol (PLA-PEG). The copolymer-ligand conjugate is added to the polymer/drug emulsion, where the ligand-conjugated copolymer spontaneously localizes and orients at the interface. Finally, the organic solvent is removed by evaporation, which results in an aqueous dispersion of polymeric nanoparticles with PEG and ligand(s) on the surface of nanoparticles (Figure 1B). Micelles formed due to the self-assembly of the copolymer are removed by extensive dilution and washing of the system. We call this method Interfacial Activity Assisted Surface Functionalization (IAASF). This technique enables the incorporation of multiple functional groups, including hydrophilic polymers and targeting ligands, on drug-loaded nanoparticles in a single step. In the current study, using folic acid and biotin as model ligands, we demonstrate the utility of IAASF technique in fabricating polymeric nanoparticles for targeted drug delivery.

2. Materials and Methods

2.1 Materials

The polymer poly(D,L-lactide-*co*-glycolide) (lactide-to-glycolide ratio of 50:50 and average molecular weight of ~38 kDa; PLGA) was purchased from Absorbable Polymers (Pelham, AL). Folic acid, biotin, polyvinyl alcohol (PVA; average Mw 30,000-70,000 Da), 6-coumarin, paclitaxel, Triton-X 100, dimethyl sulfoxide (DMSO), triethylamine, dicyclohexylcarbodimide, N-hydroxy-succinimide, stannous-2-ethyl-hexonate, dicyclohexylurea, Tween-80, phosphotungstic acid, and monoclonal anti-folic acid antibody were obtained from Sigma (St. Louis, MO). α-amine-ω-hydroxy PEG was obtained from Laysan Bio, Inc (Arab, AL). MCF-7 and 4T1 cells were obtained from American Type Culture Collection (Manassas, VA) while NCI/ADR-RES was obtained from National Cancer Institute (Bethesda, M). 300-mesh copper grid covered with Formvar/carbon was obtained from Ted Pella Inc (Redding, CA). Dichloromethane, diethyl ether, methylene choride, chloroform, methanol and toluene were obtained from Fisher Scientific (Pittsburgh, PA). Goat anti-mouse IgG-coated gold particles (25nm) and streptavidin-coated gold particles (10 nm) were obtained

from Electron Microscopy Sciences (Hatfield, PA). RPMI-1640, penicillin/streptomycin, fetal bovine serum and Trypsin-EDTA solution were obtained from Invitrogen Corporation (Carlsbad, CA). Tris-EDTA buffer was received from Promega (Madison, WI).

2.2 Methods

2.2.1 Preparation of PLA-PEG-folic acid and PLA-PEG-biotin polymer conjugates—

PLA-PEG-folic acid and PLA-PEG-biotin were synthesized using previously reported synthetic schemes with some modifications [11].

Synthesis of NHS-folic Acid and NHS-biotin: Folic acid (1.0 g) was added to a mixture of anhydrous dimethyl sulfoxide (DMSO, 40 ml) and triethylamine (TEA, 0.5 ml), and was stirred under anhydrous conditions in dark overnight. The above solution was then mixed with dicyclohexylcarbodimide (DCC, 0.5 g) and N-hydroxysuccinimide (NHS, 0.28 g), and stirred in dark for further 18 hrs. The side product dicyclohexylurea (DCU) precipitate was removed by filtration. DMSO and TEA were evaporated under vacuum. NHS-biotin was prepared similarly.

Preparation of biotin-PEG-OH and folic acid-PEG-OH: α-amine-ω-hydroxy PEG (0.2 g; average molecular weight of 3,400 Da) was dissolved in acetonitrile (0.4 ml). Methylene chloride (0.2 ml) and TEA (16 μl) were added to the above solution and stirred for 1 min. NHS-biotin or NHS-folic acid (0.05 g) was introduced to the above reaction mixture and stirred overnight under nitrogen. The reaction was stopped by the slow addition of diethyl ether (10-15 ml) to precipitate the polymer and to separate the unreacted PEG. Precipitated polymer was filtered and washed with diethyl ether. The polymer was then dissolved in hot 2-propanol (20-25 ml, 70° C), which resulted in an opaque, cloudy solution. This polymer was reprecipitated by cooling and the unconjugated folic acid and biotin molecules were removed by dialysis (Spectra/por® dialysis membrane, MWCO 1000). The dialyzed product was lyophilized and then analyzed for biotin and folic acid conjugation by ^{1}H NMR spectroscopy.

Preparation of PLA-PEG-Biotin and PLA-PEG-Folic acid: Graft polymerization of lactide onto folic acid-PEG-OH or biotin-PEG-OH was done by solvent polymerization technique. Glasswares were silanized by rinsing with a 5% methyl tri-chlorosilane solution in toluene, followed by rinsing with acetone, and then left overnight to dry at 130° C. Folic acid-PEG-OH or biotin-PEG-OH (90 mg) and L-lactide (460 mg) were added into a round bottom flask and diluted with 30 ml of toluene. The flask was placed in a desiccator and heated to 60° C until the contents dissolved. To remove traces of moisture present in the conjugate, about 70% of the added toluene was removed by distillation in a reaction vessel equipped with a Dean-Stark trap. Then, stannous 2 ethyl-hexanoate in toluene (25 mg in 0.2 ml) was added to the above reaction mixture and refluxed at 110° C for 4 hrs under nitrogen. Residual solvent was removed under vacuum using a rotary evaporator. The remaining viscous material was heated to 140° C for 1 hr under nitrogen. The reaction mixture was cooled and dissolved in 10-15 ml dichloromethane. This polymer solution was then added slowly to a stirred solution of chilled diethyl ether. The final polymer conjugate was isolated by vacuum filtration and then lyophilized. The final conjugation step was verified by ^{1}H NMR spectroscopy. The molecular weight and molecular weight distribution of the copolymer was determined by gel permeation chromatography using polystyrene standards. A Waters 717 Plus autosampler connected to a Waters 590 pump running THF as the mobile phase at a flow rate of 1 ml/min was used. Both ultraviolet-visible and refractive index detectors were used. M_w of the synthesized PLA-PEG copolymer was 12.2×10^3 Da and the polydispersity index was 1.28.

2.2.2 Preparation of surface-functionalized PLGA nanoparticles by IAASF technique—

PLGA (30 mg) was dissolved in 1 ml chloroform. An oil-in-water emulsion was

formed by emulsifying the polymer solution in 6 ml of 2.5% w/v aqueous PVA solution by using a probe sonicator (Sonicator® XL, Misonix, NY) for 5 minutes over an ice bath. The diblock copolymer PLA-PEG conjugated to either folic acid or biotin was dissolved in chloroform (8 mg in 100 μl) and added to the above emulsion with stirring. The emulsion was then stirred for 18 h at ambient conditions followed by for 2 h under vacuum to remove chloroform. Nanoparticles were recovered by ultracentrifugation (148,000 × *g* for 35 min at 4° C, Optima™ LE-80K, Beckman, Palo Alta, CA), washed three times with deionized water to remove excess PVA and to dilute the micelles formed due to the self-assembly of the PLA-PEG block copolymer. Nanoparticle suspension was then lyophilized (−80° C and <10 μm mercury pressure, Labconco, FreeZone 4.5, Kansas City, MO). To prepare paclitaxel loaded nanoparticles, paclitaxel (6 mg) was dissolved along with PLGA in chloroform and processed as described above. Paclitaxel loading in nanoparticles was determined by extracting nanoparticles with methanol and analyzing the methanol extract by HPLC as described previously [12]. To prepare fluorescently-labeled nanoparticles, 6-coumarin (250 μg) was dissolved along with PLGA in chloroform and processed as described above. We have previously demonstrated that the fluorescent label remains firmly attached to the PLGA matrix and does not leach out over 48 hrs when incubated with aqueous buffers or cell culture medium [13].

2.2.3 Characterization of surface functionalized nanoparticles by NMR—The incorporation of PLA-PEG-folic acid and PLA-PEG-biotin conjugates in PLGA nanoparticles was determined by ^{1}H NMR. Nanoparticle formulations (10 mg) were dissolved in NMR grade DMSO (1 ml) and analyzed using a Varian INOVA 800 MHz NMR instrument.

2.2.4 Characterization of surface functionalized nanoparticles by transmission electron microscopy (TEM)—Presence of ligands on the surface of nanoparticles was determined by TEM as previously described [14] with some modifications. Presence of folic acid was detected by incubating nanoparticles with mouse anti-folic acid antibody followed by incubation with gold (25 nm)-labeled goat anti-mouse IgG. Presence of biotin was detected by incubating nanoparticles with gold (10 nm)-labeled streptavidin. Nanoparticles were initially incubated with 10% BSA solution in PBS for 1 hr and then with folate-specific anti-folic acid monoclonal antibody produced in mouse for 1 hr. Unbound antibody was removed by washing the particles with PBS. Particles were then incubated with gold-labeled IgG for 1 hr and unbound gold particles were removed by washing with PBS twice. A drop of nanoparticle suspension was then put on the Formvar-coated copper grid, allowed to stand for 5 min, and excess liquid was wicked off. The grids were then incubated with phosphotungstic acid (0.5% w/v; pH 6.4) for 5 min. Nanoparticles were then visualized using a Philips Technai F20 microscope. A similar procedure was followed for detecting the presence of biotin using streptavidin-conjugated gold particles.

2.2.5 Quantitation of biotin molecules on nanoparticle surface—Number of biotin molecules on nanoparticle surface was determined using a commercially available biotin quantitation kit (Biotective Green, Invitrogen). This assay uses Biotective Green reagent, which consists of avidin labeled with a fluorescence dye and with quencher dye ligands occupying the biotin binding sites in avidin. The quencher dye ligand quenches the fluorescence through fluorescence resonance energy transfer. In the presence of biotin, the quencher ligand is displaced from Biotective Green reagent, yielding fluorescence proportional to the amount of added biotin. Nanoparticles without surface functionalization was used as negative control while biotinylated goat anti–mouse IgG supplied by Invitrogen was used as a positive control. The number of biotin molecules present in a known weight of nanoparticles was determined based on the protocol suggested by the manufacturer. Based on the particle size and density of

the polymer, 1 mg of nanoparticles was estimated to contain ~10^{12} particles. The results were expressed as the average (± S.D.) number of biotin molecules present on each particle.

2.2.6 Characterization of surface functionalized nanoparticles by surface plasmon resonance—Binding of biotin and folic acid on the surface of nanoparticles with streptavidin and anti-folic acid antibody, respectively, was evaluated by surface plasmon resonance [15]. Binding interactions were studied using the Biacore 3000 instrument available as a core facility at the University of Nebraska Medical Center, Omaha, NE. For biotin containing formulations, streptavidin sensor chip was docked and conditioned as suggested by the manufacturer with 3-4 minute pulses of 1 M sodium chloride in 50 mM sodium hydroxide. This was followed by injections of nanoparticles without biotin (10 mg/ml), biotin functionalized nanoparticles (10 mg/ml) and nanoparticles functionalized with both biotin and folic acid (10 mg/ml). In all the cases, nanoparticles were suspended in HBS-EP buffer by sonication for 30 seconds. Nanoparticles were held on an ice bath until injected.

In the case of folic acid functionalized nanoparticles, CM5 research grade sensor chip was used. Murine anti-folate antibody (Chemicon) was amine coupled directly to the CM5 surface using Biacore's reagents for amine coupling. The antibody was diluted to 30 μg/ml in 10 mM sodium acetate (pH 4.5), resulting in ~10,000 RUs following coupling. To avoid any nonspecific binding, HBS-EP buffer containing 1 mg/ml carboxymethyl dextran and 1 mg/ml BSA was injected over all surfaces prior to injecting nanoparticles with or without folic acid functionalization (10 mg/ml).

2.2.7 Accumulation of ligand-functionalized nanoparticles in tumor cells *in vitro* —MCF-7 (drug-sensitive), NCI-ADR (drug-resistant) and 4T1 (drug-sensitive) cells were cultured in RPMI-1640 medium (containing 10% fetal bovine serum) at 37° C and supplied with 5% CO_2. Cells were seeded in 24-well plates at a seeding density of 5×10^4 cells/well. Following attachment, cells were treated for 30 min with fluorescently-labeled nanoparticle formulations (100 μg/ml/well) with or without excess free folic acid and biotin (300 μM). The treated cells were washed with PBS twice, and then lysed with Triton-X solution in PBS (300 μl/well). Cell lysates were lyophilized and then extracted with methanol (1 ml/sample) for 4 h. The extracts were centrifuged at 5000 rpm for 10 min and the supernatants were subjected to HPLC analysis. The fluorescent label (6-coumarin) was eluted on a C8 column (Phenomenox) by using acetonitrile and sodium heptane sulfonate buffer in isocratic mode and detected using a fluorescence detector (Laballiance, Jasco, PA) at excitation and emission wavelengths of 450 nm and 490 nm, respectively [13]. Nanoparticle concentrations were determined based on 6-coumarin loading in nanoparticles, and then normalized to total cell protein content determined using Pierce protein assay kit.

2.2.8 Efficacy of paclitaxel-loaded nanoparticles in MCF-7 tumor xenograft model—MCF-7 cells were used to develop tumor xenografts in NCR-NU mice. Ovariectomized NCR-NU female mice (6-8 weeks old) were purchased from Taconic Farm (Albany, NY). All animal manipulations were performed using sterile techniques and were approved by Institutional Animal committee at Wayne State University, Detroit, MI. Mice were implanted subcutaneously with a 90-day 17-β-estradiol pellet (Innovative Research of America, Sarasota, FL) on the dorsal side before tumor cell injection. Following implantation, each animal received one to two million MCF-7 cells suspended in PBS. Tumors were allowed to grow to a size of at least 100 mm^3 in diameter before treatments were administered. Animals were injected intravenously with paclitaxel (20 mg/Kg) dissolved in cremophor® or encapsulated in different nanoparticle formulations. Animals that received cremophor or folic acid-functionalized blank nanoparticles were used as vehicle-treated controls. Tumor volumes were assessed regularly by measuring two perpendicular diameters with Vernier calipers and

using the formula $(L \times W^2)/2$ where L is the longest diameter and W is perpendicular to L. Tumor volume on the day of treatment was normalized to 100% for all groups.

2.2.9 Determination of paclitaxel in tumor samples—NCR-NU mice bearing MCF-7 tumor xenografts (~100 mm^3) were injected intravenously with different paclitaxel treatments as described before. Animals were euthanized 2 hrs post-injection and tumors were excised, homogenized and lyophilized. Extraction with tert-butyl methyl ether was used for sample preparation, and docetaxel was used as the internal standard. Paclitaxel and docetaxel were separated on a capillary HPLC system (Agilent, CA) coupled to a TSQ Quantum discovery Max triple-quadrupole mass spectrometric detector (Thermo Finnigan), equipped with an electrospray ionization source. The autosampler was maintained at 10° C and the column at 35° C. Hypersil GOLD C8 column (100 mm × 0.5 mm I.D) was used. Analytes were eluted at a flow rate of 0.1 ml/min, using isocratic mobile phase composed of 10 mM ammonium acetate (pH 4.0) and acetonitrile (70:30). Total run time was 4 min. Retention time of paclitaxel was 2.5 min. The mass spectrometer was run in electrospray positive mode and source conditions were as follows: capillary voltage, 3 kV; spray voltage, 3900 V; capillary temperature, 385 ° C; sheath gas pressure, 55L/h; source CID (collision energy), 5 and collision gas pressure, 1.0 mTorr. SRM mode detected the following transitions: m/z 854.5 --> 286.2 for paclitaxel and m/z 830.3 --> 549.1 for docetaxel to generate the standard curve. The chromatographic data were acquired and analyzed using Xcaliber software (Thermo Finnigan). Paclitaxel concentration was determined using the standard curve and was normalized to the tissue weight.

2.2.10 Statistical analyses—Generalized linear mixed effect model (mixed model) following natural log transformation of tumor volumes was used to analyze tumor growth inhibition data. In this model, the tumor volume change was considered to arise from both fixed effects and random effects. The fixed effects consisted of treatment effects and interaction between treatments and time effects. Random effects arise due to the variability in both tumor volume mean and tumor change among different mice. The differences in the slopes of the tumor growth curves were tested by Bonferroni adjustment. Differences in survival rate in treatment groups was analyzed by Kaplan-Meier survival analysis. One-way ANOVA was used to analyze differences in cellular accumulation of nanoparticles with and without ligands and to analyze differences in paclitaxel accumulation in tumor tissue *in vivo*. A probaility level of $P < 0.05$ was considered significant.

3.0 Results and Discussion

In the present work, we report a simple interfacial-activity assisted technique to fabricate ligand functionalized polymeric nanoparticles for targeted drug delivery. Nanoparticles fabricated using this technology have a polymeric matrix core, with the hydrophobic blocks of the copolymer-ligand conjugate anchoring into the polymer core and the hydrophilic blocks and ligands on the surface of nanoparticles (Figure 1B). The IAASF strategy differs from previously reported surface functionalization techniques [16, 17] in the fact that the particles formed are not micellar but are functionalized, matrix-type devices. This enables the incorporation and sustained release of small molecular weight drugs [18-20], proteins [21, 22], and nucleic acid therapeutics [18]. Self-assembled micellar systems are, in general, limited to encapsulating hydrophobic small molecules.

An important advantage of the IAASF technique is that it depends only on the interfacial activity of the block copolymer and the presence of oil/water interface. Matrix-type polymeric nanoparticles used in drug and macromolecular delivery are formulated using some modification of the emulsion solvent evaporation technique [23]. The method can thus be potentially used for a wide variety of polymers and targeting ligands. The greatest advantage of this method, however, is that it enables the incorporation of multiple ligands on the

nanoparticle surface in a single step. Incorporation of multiple ligands on the surface will enable simultaneous targeting of multiple antigens and/or receptors in the target tissue [24,25].

To demonstrate the potential of IAASF technique, we fabricated poly($_{D,L}$-lactide-*co*-glycolide) (PLGA) nanoparticles functionalized with known tumor targeting ligands, biotin and folic acid, using polyethylene glycol (PEG) as a hydrophilic spacer. Electrophoretic light scattering studies indicated that nanoparticles with or without ligands on the surface had similar anionic surface charge (see Table 1). The anionic surface charge of PLGA nanoparticles stems from the free carboxylic acid groups of the polymer present on the surface of particles [26]. It is possible that the number of carboxylic acid groups present is far greater than the number of ligand molecules present on the surface. This might explain the minimal effect of ligand incorporation on the surface charge of nanoparticles. Previous studies investigating ligand conjugation to PLGA nanoparticles also demonstrated a similar lack of effect of ligand conjugation on the surface charge of nanoparticles [27]. Incorporation of the ligands was confirmed by proton NMR, TEM, surface plasmon resonance and *in vitro* cell uptake studies.

3.1 Characterization of surface functionalized nanoparticles by ^{1}H NMR spectroscopy

The presence of PEG folic acid and/or biotin in surface functionalized PLGA nanoparticles was initially established by NMR analysis. ^{1}H NMR spectrum of PLGA NP functionalized with PLA-PEG-folic acid demonstrated the respective proton peaks for PEG (CH_2 at 3.5 ppm), PLA (CH_3 at 1.62 ppm and at CH 5.22 ppm) and folic acid (aromatic OH at 11.39 ppm, aromatic C-NH at 6.82 ppm, 1-benzene CH at 7.61 ppm, secondary NH at 7.89 ppm and 2-pyrazine CH at 8.58 ppm; figure 2A). ^{1}H NMR spectrum of biotin functionalized nanoparticles demonstrated proton peaks for PLA, PEG and biotin (NH at 6.24 and 6.31 ppm) (figure 2B). Folic acid and biotin functionalized nanoparticles demonstrated proton peaks for folic acid, biotin, PEG as well as PLA as shown in figure 2C. PLGA nanoparticles without ligand functionalization demonstrated proton peaks for lactide (from PLGA) at 5.22 ppm (CH) and ~1.5 ppm (CH_3) (figure 2D). Proton peaks of ligand-functionalized nanoparticles correlated well with the proton peaks of ligand-block copolymer conjugates (PLA-PEG-folic acid and PLA-PEG-biotin).

3.2 Characterization of ligand-functionalized nanoparticles using TEM

TEM was used to verify the presence of folic acid and biotin on the surface of nanoparticles. The presence of biotin was determined by using streptavidin-conjugated gold nanoparticles (10 nm). The presence of folic acid was determined by incubating nanoparticles with anti-folic acid antibody and then with gold-labeled secondary antibody (25 nm). As seen in figure 3A, nanoparticles that were functionalized with both biotin and folic acid were found to bind with the gold probes for both ligands, confirming the presence of the ligands on the surface of nanoparticles. Nanoparticles with only folic acid or biotin showed similar binding to their respective gold probes (figures 3B and 3C). These TEM studies further show that ligand-functionalized nanoparticles were in the 100 – 150 nm size range.

3.3 Characterization of surface functionalized nanoparticles by surface plasmon resonance

Surface plasmon resonance was used to determine whether the ligands present on the surface of nanoparticles were available for binding. These studies indicated a significant difference in binding affinity to respective targets for nanoparticles with and without ligands (figures 4A and B). A significant difference of about 200 RU was observed for nanoparticles with and without folic acid for binding to anti-folic acid antibody (figure 4A). A dramatic increase (3-5 folds) in response units (RU) was observed for biotin-functionalized nanoparticles compared to non-functionalized nanoparticles for binding to streptavidin (figure 4B). Difference in the response units observed for biotin nanoparticles and folic acid nanoparticles may be attributed to the differences in the binding affinities of biotin-streptavidin and folic acid-antibody combinations. Previous studies have shown that binding of folic acid to its target is in general

weaker ($K_D \sim 10^{-10}$ M) [28] than the binding of biotin to streptavidin ($K_D \sim 10^{-15}$ M) [29]. Presence of both biotin and folic acid on the surface resulted in slightly weaker binding for the individual ligands. Nanoparticles with biotin alone resulted in ~1340 response units for binding with streptavidin while nanoparticles with both biotin and folic acid resulted in ~1145 response units for binding with streptavidin. Reduced binding of dual-ligand nanoparticles is probably due to fewer number of biotin molecules present on the surface. Quantitative studies indicate that nanoparticles with both biotin and folic acid contain about 13.0 ± 1.4 biotin molecules per particle while biotin-only nanoparticles contain about 17.0 ± 1.6 biotin molecules per particle. Steric hindrance from folic acid may also contribute to the reduced binding of biotin on dual-ligand nanoparticles to streptavidin.

3.4 Accumulation of ligand-functionalized nanoparticles in tumor cells *in vitro*

In vitro cell uptake experiments performed with fluorescently-labeled nanoparticles [13] were used to further support the availability of surface-bound ligands for binding with their respective receptors. As shown in figure 5, ligand-conjugated nanoparticles were extensively taken up relative to nanoparticles without ligands by different cancer cell lines that overexpress receptors for these ligands. Addition of excess free ligand decreased the uptake of ligand-conjugated nanoparticles, indicating the involvement of corresponding receptors in the cellular uptake of nanoparticles [30]. Similar increase in uptake by target cells was observed for nanoparticles with just one ligand relative to nanoparticles without ligands (not shown). While these studies suggest that free folic acid and biotin in the body can interfere with the uptake of nanoparticles by tumor cells, it is important to note that the concentration of the free ligands used in this competition experiment (300 μM) was several-fold higher than physiological concentrations of the ligands (folic acid, 5 to 50 nM and biotin, 0.25 nM) [31,32].

3.5 Efficacy of paclitaxel-loaded nanoparticles in MCF-7 tumor xenograft model

The ability of ligand functionalized nanoparticles to target paclitaxel, a commonly used anticancer drug, to tumors was then evaluated *in vivo*. Incorporation of the targeting ligands did not affect the loading of the drug in nanoparticles significantly (Table 1). The effect of a single-dose paclitaxel treatment on tumor growth was investigated in nude mice bearing MCF-7 xenografts, which are known to overexpress both folate [33] and biotin [34] receptors At the dose used (20 mg/kg paclitaxel; nanoparticle dose of ~3 mg/animal), free paclitaxel and paclitaxel encapsulated in non-functionalized nanoparticles were only marginally effective (not statistically significant). Incorporation of folic acid and/or biotin resulted in enhanced tumor growth inhibition ($P<0.05$ Vs vehicle-treated; figure 6A). Interestingly, treatment with nanoparticles that had both folic acid and biotin on the surface resulted in complete tumor regression in one animal and significant inhibition in tumor growth in other animals ($P<0.05$ Vs nanoparticles with folic acid and $P = 0.06$ Vs nanoparticles with biotin). Representative pictures of tumors at the end of 18 days can be seen in figure 6B. Enhanced tumor inhibition was accompanied by increased survival in treated groups. At the end of 80 days post-treatment, 50% of animals that received folic acid and biotin functionalized nanoparticles survived ($P<0.05$ Vs vehicle-treated) while the survival rates were 40% and 20% in folic acid-functionalized nanoparticle group and biotin nanoparticle group, respectively (not shown). None of the animals survived beyond three weeks in the other groups.

3.6 Enhanced tumor accumulation of surface functionalized nanoparticles

To demonstrate greater tumor targeted paclitaxel delivery as the mechanism of enhanced tumor growth inhibition with ligand functionalized nanoparticles, we determined the tumor accumulation of paclitaxel following treatment with different paclitaxel formulations. As can be seen in figure 7, treatment with free paclitaxel or paclitaxel in nanoparticles without ligands resulted in drug concentrations that were close to the limit of detection (2 pg/ml). In this study

we used a sub-optimal dose (20 mg/kg) of paclitaxel to demonstrate the improvement in efficacy with targeted formulations while other studies have used much higher doses up to 100 mg/kg doses [35]. Treatment with folic acid or biotin functionalized nanoparticles resulted in significant drug accumulation in the tumor tissue. However, highest tumor drug accumulation was observed in animals that received nanoparticles functionalized with both folic acid and biotin, which correlates well with the enhanced therapeutic efficacy observed following treatment with dual ligand-functionalized nanoparticles.

A combination of active tumor targeting through folic acid and biotin receptors and passive targeting because of the enhanced permeation and retention (EPR) effect [4-7] could have contributed to the observed increase tumor accumulation of ligand-functionalized nanoparticles. Additionally, our previous studies have shown that PLGA nanoparticles release the encapsulated drug slowly (~55% of the encapsulated drug release in 35 days) [12]. Enhanced tumor targeting and sustained drug availability in the tumor tissue could have contributed to the enhanced tumor growth inhibition and improved animal survival observed with ligand functionalized nanoparticles. Several previous studies have examined the incorporation of different targeting ligands and the therapeutic efficacy of nanoparticle-encapsulated drugs in animal tumor models. Most of these studies utilized the conjugation of ligands to pre-synthesized nanoparticles or self-assembly of ligand-conjugated block copolymers. Depending on the ligand, the drug, the nanoparticle formulation and the tumor model used, targeting enhancements of 2 to 10-fold have been documented for ligand functionalized nanoparticles versus free drug treatment [20,27,36-38]. While a direct comparison of different ligand incorporation techniques is difficult because of the differences in the formulations and the tumor models used, we saw a similar significant increase in tumor accumulation of paclitaxel when administered in ligand-functionalized nanoparticles in our studies. The current study thus confirms the potential of the IAASF technology for fabricating ligand functionalized nanoparticles for targeted drug delivery.

4.0 Conclusion

We have described a surface-functionalization methodology for polymeric nanoparticles that is adaptable to a wide variety of polymer platforms, therapeutic agents and targeting ligands. The IAASF technique enables the incorporation of multiple ligands on nanoparticle surface in a single step. Ligand functionalization significantly enhanced nanoparticle accumulation in tumor cells *in vitro*, and resulted in improved efficacy of paclitaxel-loaded nanoparticles in a mouse xenograft tumor model. We expect that this new surface functionalization technique will enable efficient fabrication of multifunctional nanoparticles for targeted delivery of different therapeutic agents.

Acknowledgements

Funding from NIH (7R21CA116641-02). We thank Barbara J M Booth at the Molecular Interaction Core Facility, University of Nebraska Medical Center, Omaha, NE, for assistance with surface plasmon analysis. We thank Alice Resseler at the Characterization Facility, University of Minnesota, Minneapolis, MN, for assistance with TEM studies.

References

1. Allen TM. Ligand-targeted therapeutics in anticancer therapy. Nat Rev Cancer 2002;2:750–763. [PubMed: 12360278]
2. Allen TM, Cullis PR. Drug delivery systems: entering the mainstream. Science 2004;303:1818–1822. [PubMed: 15031496]
3. Langer R. Drug delivery and targeting. Nature 1998;392:5–10. [PubMed: 9579855]
4. Duncan R. The dawning era of polymer therapeutics. Nat Rev Drug Discov 2003;2:347–360. [PubMed: 12750738]

5. Otsuka H, Nagasaki Y, Kataoka K. PEGylated nanoparticles for biological and pharmaceutical applications. Adv Drug Deliv Rev 2003;55:403–419. [PubMed: 12628324]
6. Torchilin VP. Micellar nanocarriers: pharmaceutical perspectives. Pharm Res 2007;24:1–16. [PubMed: 17109211]
7. Wang MD, Shin DM, Simons JW, Nie S. Nanotechnology for targeted cancer therapy. Expert Rev Anticancer Ther 2007;7:833–837. [PubMed: 17555393]
8. Gref R, Couvreur P, Barratt G, Mysiakine E. Surface-engineered nanoparticles for multiple ligand coupling. Biomaterials 2003;24:4529–4537. [PubMed: 12922162]
9. Popielarski SR, Pun SH, Davis ME. A Nanoparticle-Based Model Delivery System To Guide the Rational Design of Gene Delivery to the Liver. 1. Synthesis and Characterization. Bioconjug Chem 2005;16:1063–1070. [PubMed: 16173781]
10. Sahoo SK, Ma W, Labhasetwar V. Efficacy of transferrin-conjugated paclitaxel-loaded nanoparticles in a murine model of prostate cancer. Int J Cancer 2004;112:335–340. [PubMed: 15352049]
11. Salem AK, Cannizzaro SM, Davies MC, Tendler SJ, Roberts CJ, Williams PM, et al. Synthesis and characterisation of a degradable poly(lactic acid)-poly(ethylene glycol) copolymer with biotinylated end groups. Biomacromolecules 2001;2:575–580. [PubMed: 11749223]
12. Chavanpatil MD, Patil Y, Panyam J. Susceptibility of nanoparticle-encapsulated paclitaxel to P-glycoprotein-mediated drug efflux. Int J Pharm 2006;320:150–156. [PubMed: 16713148]
13. Panyam J, Sahoo SK, Prabha S, Bargar T, Labhasetwar V. Fluorescence and electron microscopy probes for cellular and tissue uptake of poly(D,L-lactide-co-glycolide) nanoparticles. Int J Pharm 2003;262:1–11. [PubMed: 12927382]
14. Debotton N, Parnes M, Kadouche J, Benita S. Overcoming the formulation obstacles towards targeted chemotherapy: in vitro and in vivo evaluation of cytotoxic drug loaded immunonanoparticles. J Control Release 2008;127:219–230. [PubMed: 18343522]
15. Sonvico F, Mornet S, Vasseur S, Dubernet C, Jaillard D, Degrouard J, et al. Folate-conjugated iron oxide nanoparticles for solid tumor targeting as potential specific magnetic hyperthermia mediators: synthesis, physicochemical characterization, and in vitro experiments. Bioconjug Chem 2005;16:1181–1188. [PubMed: 16173796]
16. Farokhzad OC, Jon S, Khademhosseini A, Tran TNT, LaVan DA, Langer R. Nanoparticle-Aptamer Bioconjugates: A New Approach for Targeting Prostate Cancer Cells. Cancer Res 2004;64:7668–7672. [PubMed: 15520166]
17. Gu F, Zhang L, Teply BA, Mann N, Wang A, Radovic-Moreno AF, et al. Precise engineering of targeted nanoparticles by using self-assembled biointegrated block copolymers. Proc Natl Acad Sci 2008;105:2586–2591. [PubMed: 18272481]
18. Panyam J, Zhou WZ, Prabha S, Sahoo SK, Labhasetwar V. Rapid endo-lysosomal escape of poly (DL-lactide-co-glycolide) nanoparticles: implications for drug and gene delivery. FASEB J 2002;16:1217–1226. [PubMed: 12153989]
19. Sahoo SK, Ma W, Labhasetwar V. Efficacy of transferrin-conjugated paclitaxel-loaded nanoparticles in a murine model of prostate cancer. Int J Cancer 2004;112:335–340. [PubMed: 15352049]
20. Sun B, Ranganathan B, Feng SS. Multifunctional poly(D,L-lactide-co-glycolide)/montmorillonite (PLGA/MMT) nanoparticles decorated by Trastuzumab for targeted chemotherapy of breast cancer. Biomaterials 2008;29:475–486. [PubMed: 17953985]
21. Lee SH, Zhang Z, Feng SS. Nanoparticles of poly(lactide)--tocopheryl polyethylene glycol succinate (PLA-TPGS) copolymers for protein drug delivery. Biomaterials 2007;28:2041–2050. [PubMed: 17250886]
22. Shen H, Ackerman AL, Cody V, Giodini A, Hinson ER, Cresswell P, et al. Enhanced and prolonged cross-presentation following endosomal escape of exogenous antigens encapsulated in biodegradable nanoparticles. Immunology 2006;117:78–88. [PubMed: 16423043]
23. Panyam J, Labhasetwar V. Biodegradable nanoparticles for drug and gene delivery to cells and tissue. Adv Drug Deliv Rev 2003;55:329–347. [PubMed: 12628320]
24. Saul JM, Annapragada AV, Bellamkonda RV. A dual-ligand approach for enhancing targeting selectivity of therapeutic nanocarriers. J Control Release 2006;114:277–287. [PubMed: 16904220]

25. Sawant RM, Hurley JP, Salmaso S, Kale A, Tolcheva E, Levchenko TS, et al. "SMART" drug delivery systems: double-targeted pH-responsive pharmaceutical nanocarriers. Bioconjug Chem 2006;17:943–949. [PubMed: 16848401]
26. Cegnar M, Kos J, Kristl J. Cystatin incorporated in poly(lactide-co-glycolide) nanoparticles: development and fundamental studies on preservation of its activity. Eur J Pharm Sci 2004;22:357–364. [PubMed: 15265505]
27. Kocbek P, Obermajer N, Cegnar M, Kos J, Kristl J. Targeting cancer cells using PLGA nanoparticles surface modified with monoclonal antibody. J Control Release 2007;120:18–26. [PubMed: 17509712]
28. Lu Y, Sega E, Leamon CP, Low PS. Folate receptor-targeted immunotherapy of cancer: mechanism and therapeutic potential. Adv Drug Deliv Rev 2004;56:1161–1176. [PubMed: 15094213]
29. Laitinen OH, Nordlund HR, Hytonen VP, Uotila ST, Marttila AT, Savolainen J, et al. Rational design of an active avidin monomer. J Biol Chem 2003;278:4010–4014. [PubMed: 12458212]
30. Yoo HS, Park TG. Folate receptor targeted biodegradable polymeric doxorubicin micelles. J Control Release 2004;96:273–283. [PubMed: 15081218]
31. Kimura M, Umegaki K, Higuchi M, Thomas P, Fenech M. Methylenetetrahydrofolate reductase C677T polymorphism, folic acid and riboflavin are important determinants of genome stability in cultured human lymphocytes. J Nutr 2004;134:48–56. [PubMed: 14704292]
32. Mock DM, Lankford GL, Mock NI. Biotin accounts for only half of the total avidin-binding substances in human serum. J Nutr 1995;125:941–946. [PubMed: 7722698]
33. Lee ES, Na K, Bae YH. Doxorubicin loaded pH-sensitive polymeric micelles for reversal of resistant MCF-7 tumor. J Control Release 2005;103:405–418. [PubMed: 15763623]
34. Lee ES, Na K, Bae YH. Super pH-sensitive multifunctional polymeric micelle. Nano Lett 2005;5:325–329. [PubMed: 15794620]
35. Zhang X, Burt HM, Von Hoff D, Dexter D, Mangold G, Degen D, et al. An investigation of the antitumour activity and biodistribution of polymeric micellar paclitaxel. Cancer Chemother Pharmacol 1997;40:81–86. [PubMed: 9137535]
36. Farokhzad OC, Cheng J, Teply BA, Sherifi I, Jon S, Kantoff PW, et al. Targeted nanoparticle-aptamer bioconjugates for cancer chemotherapy in vivo. Proc Natl Acad Sci U S A 2006;103:6315–6320. [PubMed: 16606824]
37. Kukowska-Latallo JF, Candido KA, Cao Z, Nigavekar SS, Majoros IJ, Thomas TP, et al. Nanoparticle targeting of anticancer drug improves therapeutic response in animal model of human epithelial cancer. Cancer Res 2005;65:5317–5324. [PubMed: 15958579]
38. Zhang Z, Huey Lee S, Feng SS. Folate-decorated poly(lactide-co-glycolide)-vitamin E TPGS nanoparticles for targeted drug delivery. Biomaterials 2007;28:1889–1899. [PubMed: 17197019]

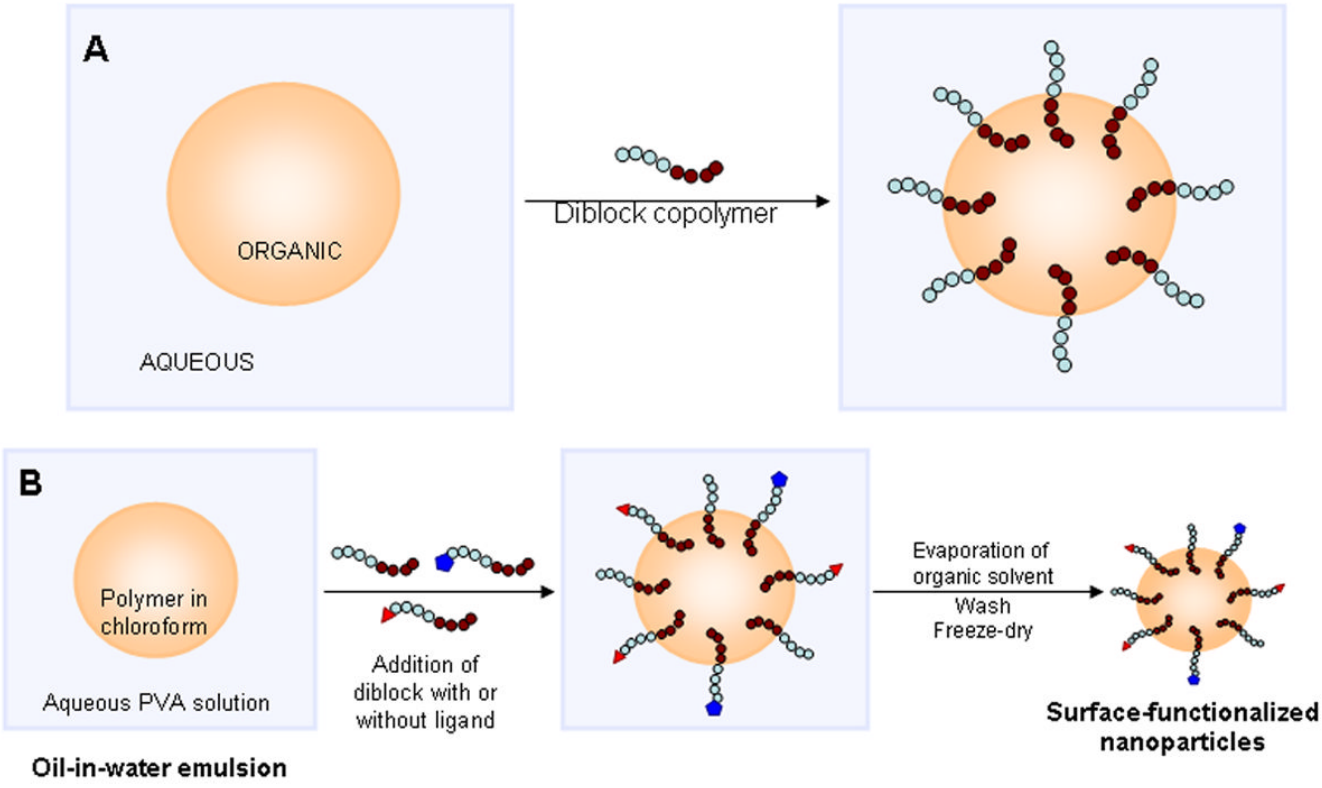

Figure 1.

(A) Behavior of amphiphilic diblock copolymer in an oil/water biphasic system. **(B)** Introduction of PLA-PEG and PLA-PEG-ligand conjugates during the emulsification step results in nanoparticles with PEG and PEG-ligand on nanoparticle surface. Hydrophobic blocks (for example, PLA) are shown as a series of brown circles while hydrophilic blocks (for example, PEG) are shown as a series of blue circles.

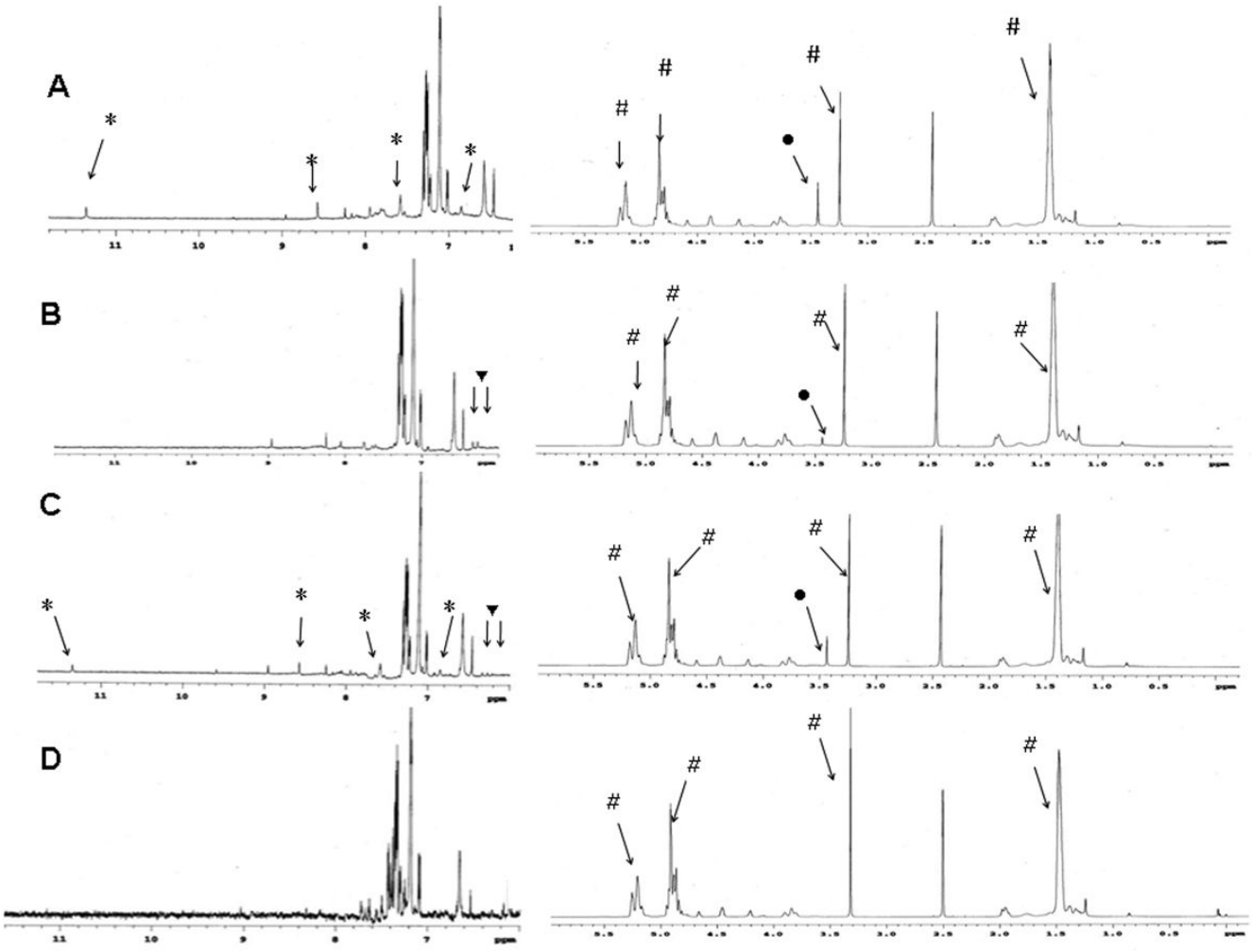

Figure 2.
Proton NMR of PLGA nanoparticles surface functionalized with **(A)** PLA-PEG-folic acid; **(B)** PLA-PEG-biotin; **(C)** PLA-PEG-folic acid and PLA-PEG-biotin. **(D)** NMR spectrum for PLGA nanoparticles without any ligands is shown as a control. Legend: PLGA proton peaks (#); PEG proton peaks (●); FA proton peaks (*) and BI proton peaks (▼)

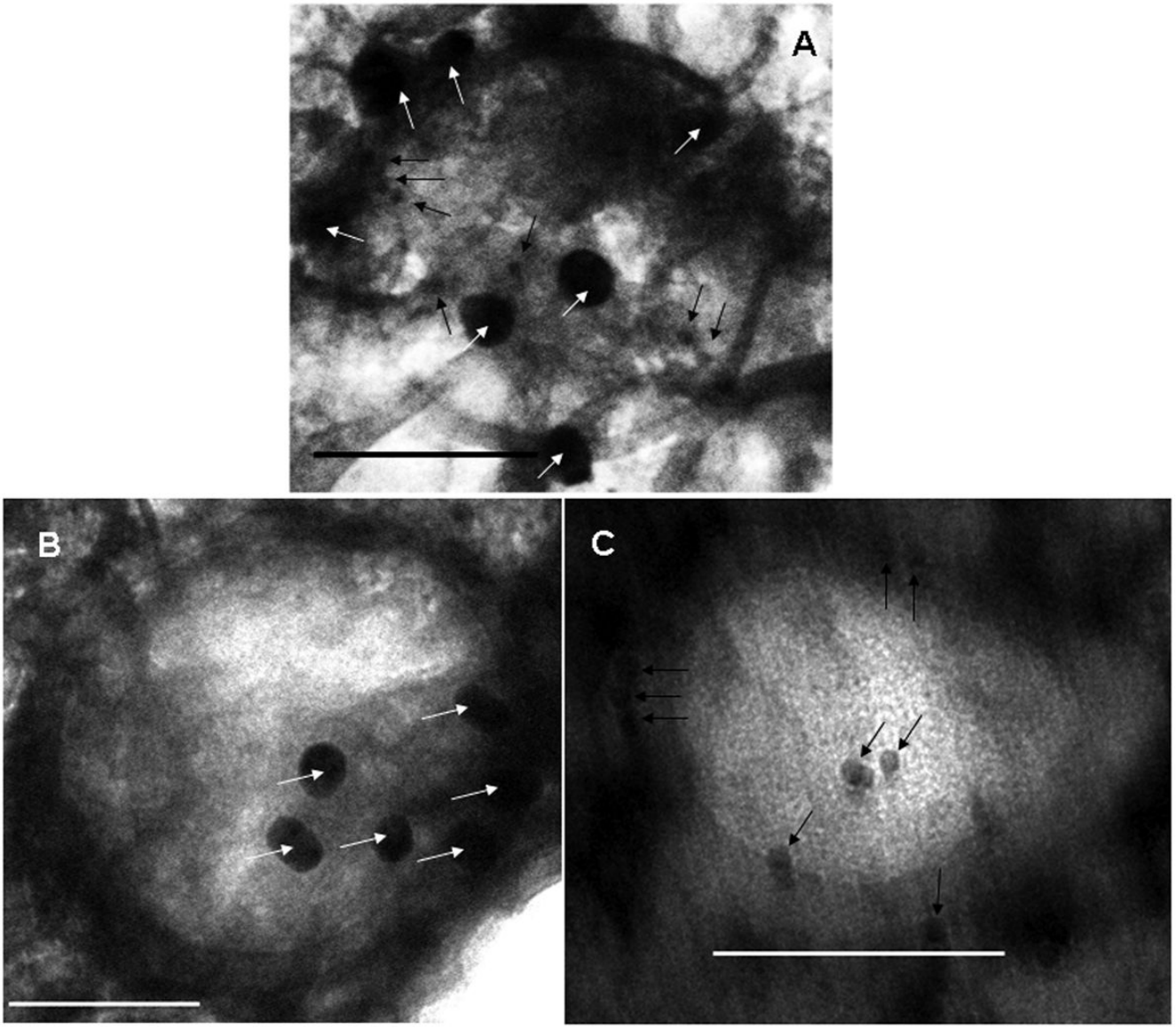

Figure 3.

TEM studies demonstrating the presence of folic acid and biotin on nanoparticles. **(A)** Dual-ligand nanoparticles were incubated with anti-folic acid antibody and then with secondary antibody conjugated to 25 nm gold particles (indicated by white arrows) and streptavidin-conjugated 10 nm gold particles (indicated by black arrows). **(B)** Folic acid functionalized nanoparticles were incubated with anti-folic acid antibody and then with secondary antibody conjugated to 25 nm gold particles (indicated by white arrows). **(C)** Biotin-functionalized nanoparticles were incubated with streptavidin-conjugated 10 nm gold particles (indicated by black arrows). In **A**, **B** and **C**, bar is 100 nm.

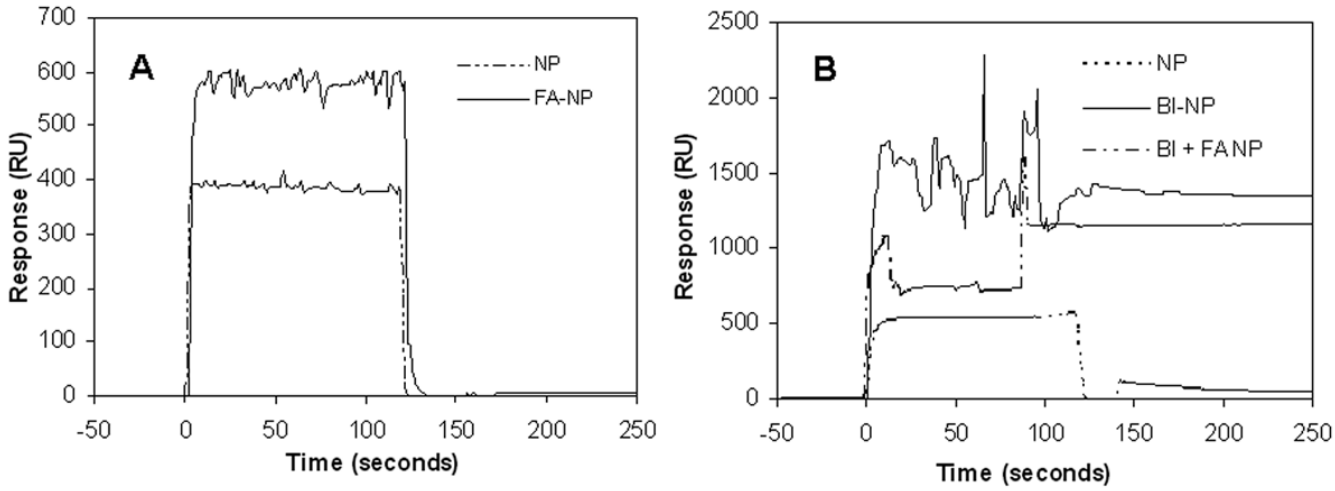

Figure 4.

Surface plasmon resonance-based binding analysis of ligand-functionalized nanoparticles. **(A)** Binding of folic acid functionalized nanoparticles (FA-NP) and non-functionalized nanoparticles (NP) to anti-folate antibody coated sensor chip. **(B)** Binding of biotin functionalized nanoparticles (BI-NP), dual functionalized nanoparticles (BI+FA NP) and non-functionalized nanoparticles (NP) to streptavidin-coated sensor chip.

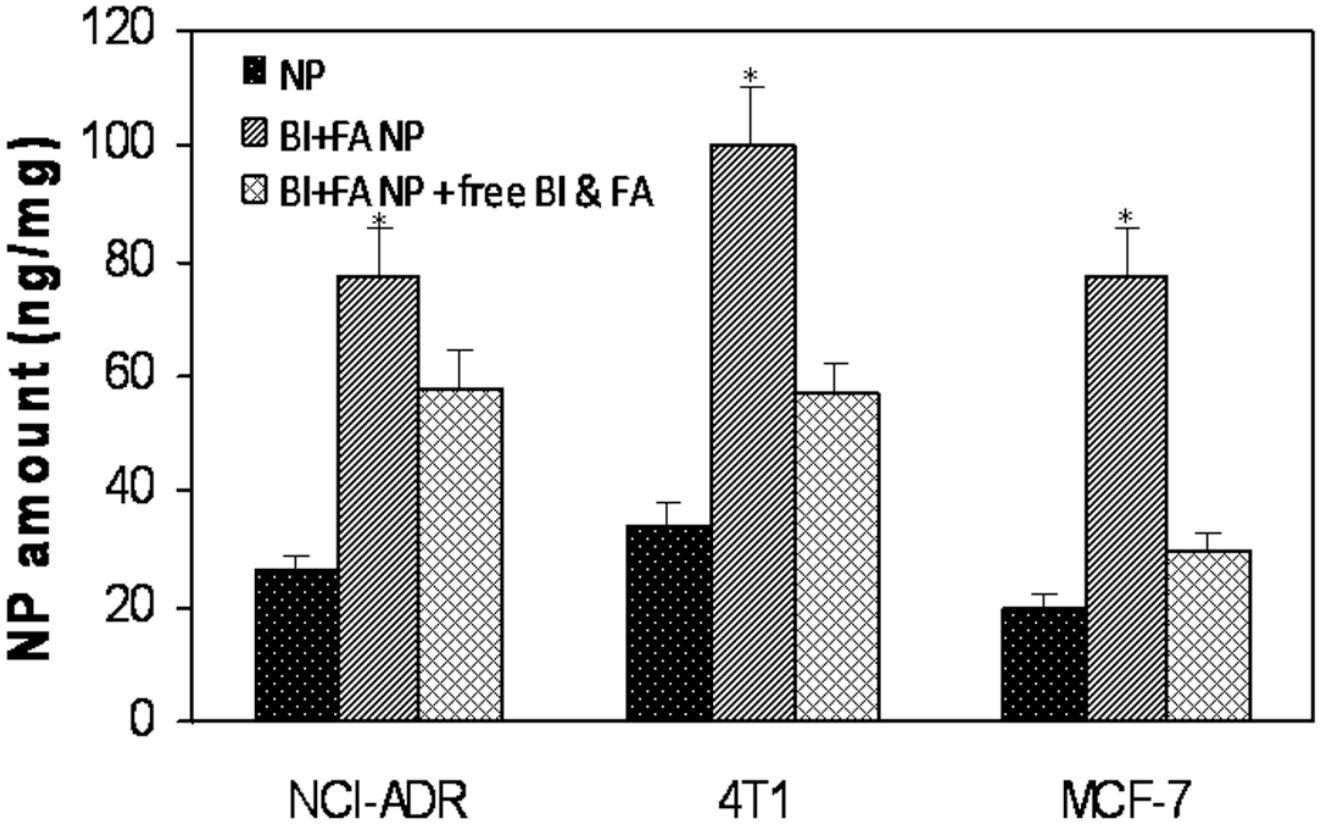

Figure 5.
Effect of folic acid and biotin incorporation on nanoparticle accumulation in different breast cancer cells. Cells were grown on 24-well plates and incubated with nanoparticles in the presence or absence of excess free ligands. Accumulation of nanoparticle-associated fluorescent label was determined by HPLC and the data was normalized to the total cell protein. Data as mean ± SD (n = 6). *P<0.05 Vs other groups.

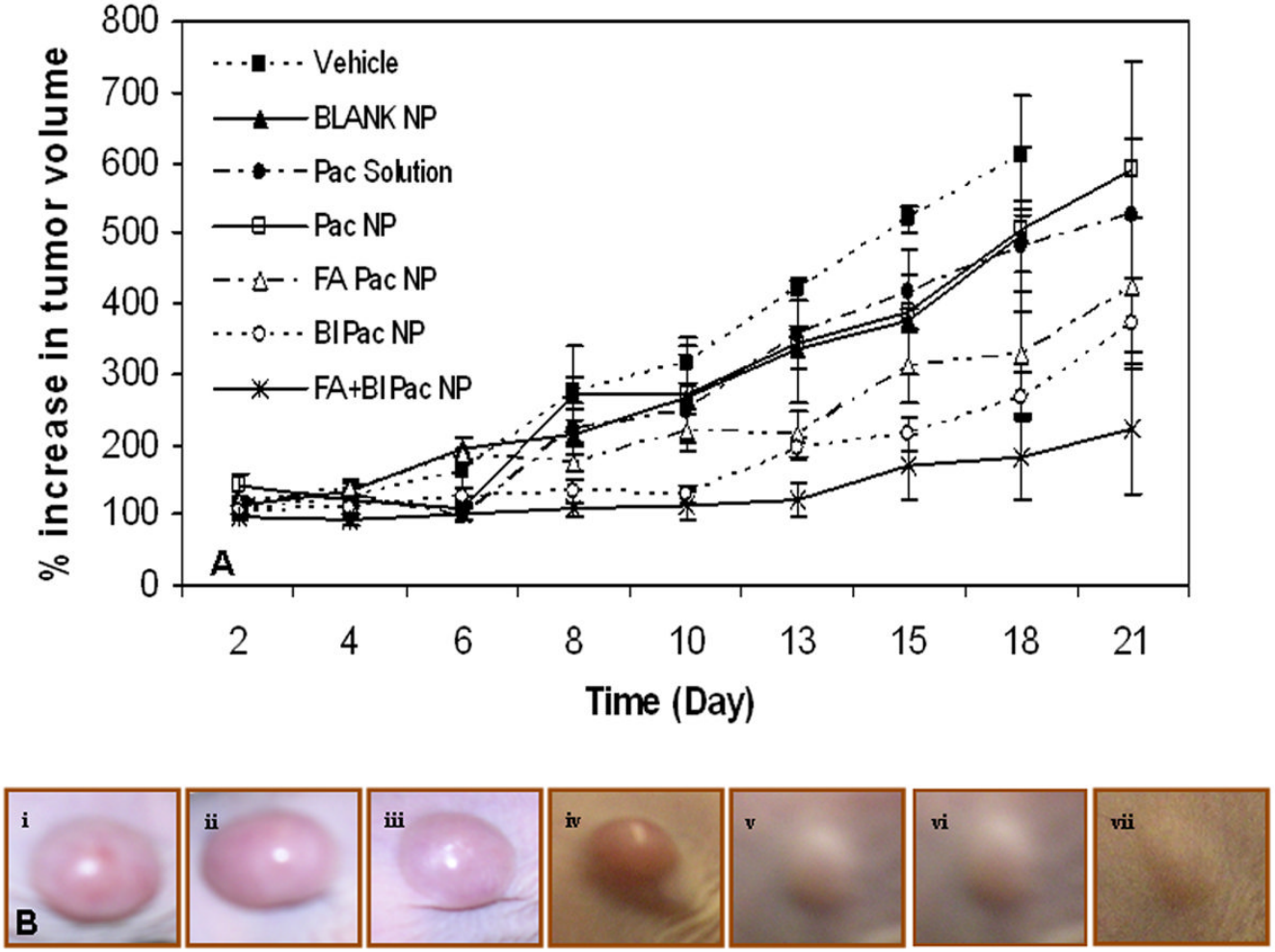

Figure 6.

Incorporation of PEG-folic acid and/or PEG-biotin on nanoparticle surface results in enhanced anti-cancer effectiveness of nanoparticle-encapsulated paclitaxel. NCR-NU mice bearing MCF-7 xenografts were injected with paclitaxel (20 mg/Kg) in solution or encapsulated in nanoparticles (~3 mg/animal) with or without surface functionalization. **(A)** Growth in tumor volume was determined over a period of 21 days. Data as mean ± SD (n = 6). **(B)** Representative pictures of tumors in animals that received i) Vehicle, ii) Blank NP, iii) Pac solution, iv) Pac NP, v) FA Pac NP, vi) BI Pac NP and vii) FA+BI Pac NP.

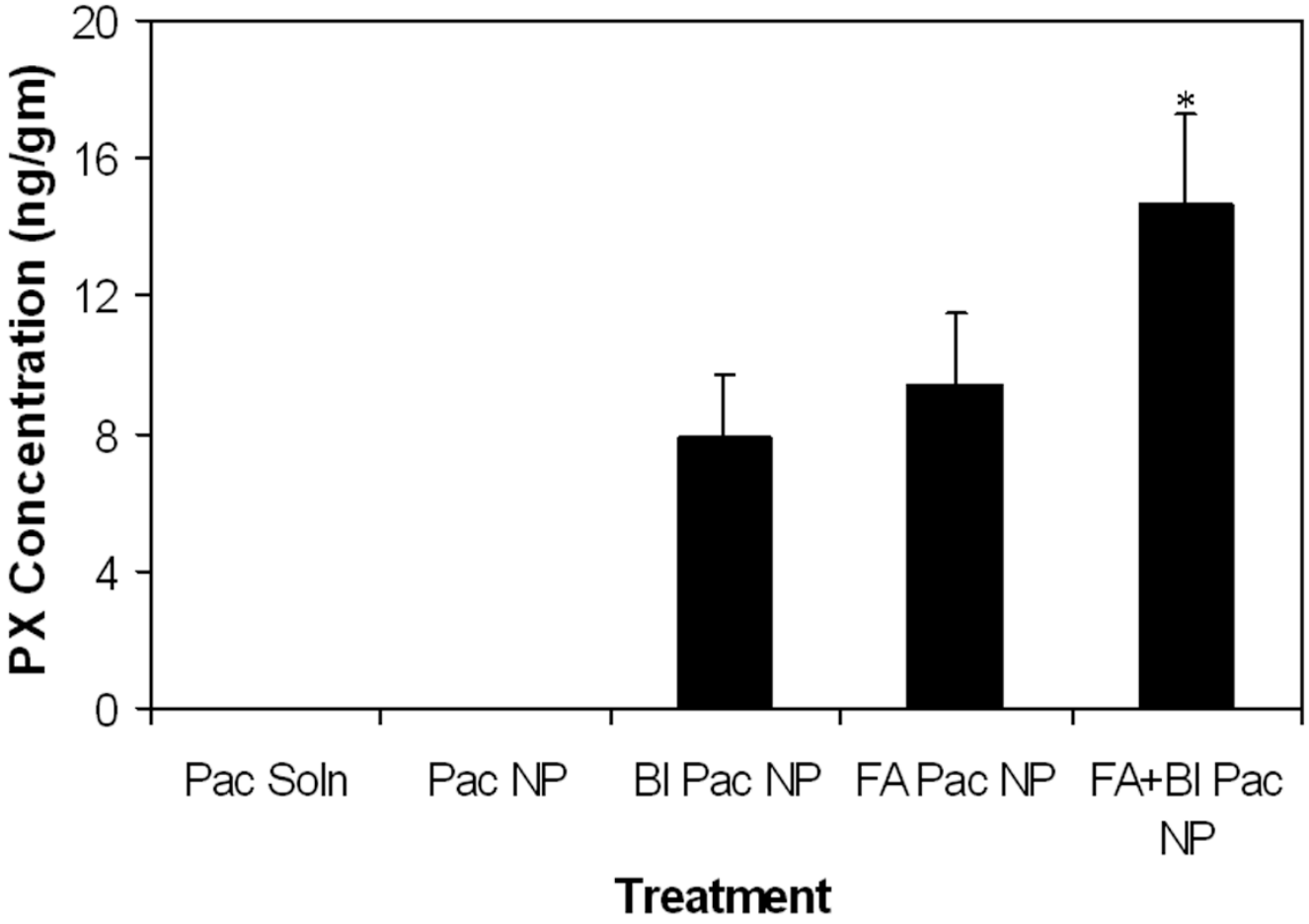

Figure 7.

Effect of ligand functionalization on tumor accumulation of paclitaxel. NCR-NU mice bearing MCF-7 xenografts were injected with paclitaxel (20 mg/Kg) in solution or encapsulated in nanoparticles (~3 mg/animal) with or without surface functionalization. Animals were euthanized 2 hrs post treatment and paclitaxel concentration in the tumor tissue was determined by LC-MS/MS. Data as mean ± SD (n = 4). *P < 0.05 versus other treatment groups.

Table 1

Characterization of surface functionalized nanoparticles

Formulation	Zeta potential (mV)	Paclitaxel loading (% w/w)	Loading efficiency (%)
Control nanoparticles	-12.6 ± 0.2	12.0 ± 0.3	80 ± 2
Folic acid functionalized	-16.8 ± 0.3	11.9 ± 0.5	80 ± 3
Biotin functionalized	-12.1 ± 0.3	13.8 ± 0.5	92 ± 3
Folic acid and biotin functionalized	-14.8 ± 0.6	13.8 ± 0.5	92 ± 2